# CAD-Oriented Fullwave Equivalent Circuit Models for Waveguide Components and Circuits

Andreas Weisshaar, *Member, IEEE,* Mauro Mongiardo, *Member, IEEE,* Alok Tripathi, *Student Member, IEEE,* and Vijai K. Tripathi, *Fellow, IEEE*

***Abstract*—New multimode equivalent circuit models for single and cascaded $E$-plane and $H$-plane step discontinuities in rectangular waveguides are presented. The computer-aided design (CAD)-oriented equivalent circuit models enable rigorous and efficient fullwave analysis of waveguide components and circuits entirely by circuit simulation. The method has been implemented on the microwave circuit simulator Libra and applied to waveguide structures containing single and cascaded irises and stub discontinuities. Comparisons of circuit simulation results for single and cascaded inductive irises as well as a single and three $E$-plane stubs with the standard mode-matching method show perfect agreement. Results of a Ka-band bandpass filter analysis are in good agreement with a mode-matching solution that includes the correct edge condition.**

## I. Introduction

COMPUTER-AIDED design (CAD) of waveguide filters and components generally requires use of a rigorous fullwave analysis technique such as the finite-element or finite-difference method, or the mode-matching method. Although general purpose tools like, for example, fullwave finite-element solvers [1] are commercially available, modal analysis methods are often preferred since they are computationally more efficient [2]–[4] and provide physical insight [5]. However, available modal analysis tools are typically standalone programs which are often developed for a particular type of problem.

In this paper, rigorous CAD-oriented fullwave equivalent circuit models for single and cascaded $E$-plane and $H$-plane step discontinuities in rectangular waveguides are proposed. With these novel multimode equivalent circuit representations, a large class of waveguide components and circuits, including filters and phase shifters, can be analyzed and designed entirely with commercial circuit simulators. Since the equivalent circuit models are derived from a modal analysis, a fullwave analysis can be performed directly by *circuit simulation* thus eliminating the need for additional matrix inversion.

In the following sections, equivalent circuit models of single and cascaded $E$-plane and $H$-plane step discontinuities, which form the basic building blocks of many waveguide components, are presented. In particular, the accuracy of the circuit simulation is demonstrated for both interacting and noninteracting steps. As an example of a practical application of the new circuit model approach, a comparison of a waveguide filter analysis by circuit simulation on Libra [6] and standard mode-matching simulation [3], [7], including the correct edge behavior [8] is shown.

Manuscript received March 29, 1996; revised August 5, 1996. M. Mongiardo was supported in part by Centro Nazionale delle Ricerche (CNR).

A. Weisshaar, A. Tripathi, and V. K. Tripathi are with the Department of Electrical and Computer Engineering, Oregon State University, Corvallis, OR 97331 USA.

M. Mongiardo is with the Istituto di Elettronica, Universitá di Perugia, I-06100, Perugia, Italy.

Publisher Item Identifier S 0018-9480(96)08522-5.

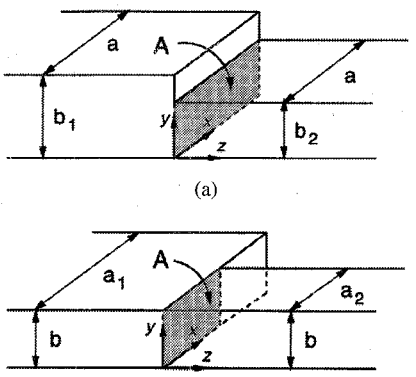


Fig. 1. Geometry of (a) an $E$-plane step and (b) an $H$-plane step discontinuity in a rectangular waveguide.

## II. Multimode Equivalent Circuit Models

The $E$-plane and $H$-plane step discontinuities in a rectangular waveguide are illustrated in Fig. 1. The multimode equivalent circuit representations of the fullwave step discontinuity problem can be derived directly from a modal analysis, as shown below.

### A. Modal Analysis

Assuming $TE_{10}$ mode incidence on the discontinuity, the reflected and transmitted waves are described in terms of $TE_{m0}$ modes ($m = 1, 2, 3, \cdots$) for $H$-plane steps and $LSE_{1n}$ modes ($n = 0, 1, 2, \cdots$) for $E$-plane steps, respectively [9], [10]. The transverse electric field, $E_y$, and transverse magnetic field component, $H_x$, in each waveguide can be expressed in terms of expansions in the normalized transverse modal fields [5]. They are given in waveguide $I$ by

$$E_y^I(x, y, z) = \sum_{m=1}^{M} V_m^I(z)\phi_m^I(x, y)$$

$$H_x^I(x, y, z) = -\sum_{m=1}^{M} I_m^I(z)\phi_m^I(x, y) \qquad (1)$$

and in waveguide $II$ by

$$E_y^{II}(x, y, z) = \sum_{n=1}^{N} V_n^{II}(z)\phi_n^{II}(x, y)$$

$$H_x^{II}(x, y, z) = -\sum_{n=1}^{N} I_n^{II}(z)\phi_n^{II}(x, y). \tag{2}$$

$V_k^{I,II}(z)$ and $I_k^{I,II}(z)$ are the total voltage and current amplitudes of mode $k$ in waveguide $I$ and $II$, respectively, and, in general, comprise both the incident and reflected waves. The orthonormal sets of transverse field solutions $\phi_m^{I,II}(x, y)$ for $TE_{m0}$ modes [13] and $\phi_n^{I,II}(x, y)$ for $LSE_{1,n-1}$ modes ($n = 1, 2, 3, \cdots$) are given in the Appendix.[1] The expansions in (1) and (2) have been truncated to $M$ modes in waveguide $I$ and $N$ modes in waveguide $II$. In order to avoid relative convergence problems [3], [11], the number of expansion terms, $M$ and $N$, is typically chosen such that $M/N$ is as close as possible to the corresponding ratio in waveguide height $b_1/b_2$ for $E$-plane steps or waveguide width, $a_1/a_2$, for $H$-plane steps, respectively.

The continuity of the transverse fields at the discontinuity at $z = 0$ yields for the electric field

$$E_y^I(x, y, 0) = \begin{cases} 0, & \text{on conducting boundary} \\ E_y^{II}(x, y, 0), & \text{on aperture A} \end{cases} \tag{3}$$

and for the magnetic field

$$H_x^I(x, y, 0) = H_x^{II}(x, y, 0) \qquad \text{on aperture A}. \tag{4}$$

Following the mode-matching procedure as described in [3] and [7], two systems of linear equations relating the voltage and current amplitude coefficients in each waveguide are found as

$$V_m^I = \sum_{n=1}^{N} C_{mn} V_n^{II}, \qquad (m = 1, \cdots, M) \tag{5}$$

and

$$I_n^{II} = \sum_{m=1}^{M} C_{mn} I_m^I, \qquad (n = 1, \cdots, N). \tag{6}$$

Equations (5) and (6) may be expressed compactly in matrix form as

$$\mathbf{V}^I = \mathbf{C}\mathbf{V}^{II}$$
$$\mathbf{I}^{II} = \mathbf{C}^T\mathbf{I}^I \tag{7}$$

with the superscript $T$ denoting transposition [3] and [7]. The coefficients $C_{mn}$ are the mode-coupling (overlap) integrals given by

$$C_{mn} = \int_A \phi_m^I(x, y)\phi_n^{II}(x, y)\, dx\, dy. \tag{8}$$

Note that the coupling coefficients are different for $H$-plane and $E$-plane steps (see the Appendix).

It is noted that the conventional modal description of step discontinuities in terms of incident and reflected waves does not directly render CAD-oriented equivalent circuit representations. In contrast, (5) and (6) for total voltage and current amplitudes lead to a simple network description of the step discontinuity: voltages in waveguide $I$ are controlled by voltages in waveguide $II$, and currents in waveguide $II$ are controlled by currents in waveguide $I$. The corresponding equivalent circuit representation of the step discontinuity is shown in Fig. 2. It consists of linear voltage-controlled voltage sources and current-controlled current sources, which is similar to the network description of coupled transmission lines [12]. Higher order modes are represented by their modal impedances, i.e.,

$$Z_m^{I,II} = \frac{j\omega\mu}{\sqrt{\left(\frac{m\pi}{a_{1,2}}\right)^2 - \omega^2\mu\epsilon}} \tag{9}$$

for $TE_{m0}$ modes [13], and

$$Z_n^{I,II} = \frac{\sqrt{\left(\frac{\pi}{a}\right)^2 + \left[\frac{(n-1)\pi}{b_{1,2}}\right]^2 - \omega^2\mu\epsilon}}{j\omega\epsilon} \cdot \frac{\omega^2\mu\epsilon}{\omega^2\mu\epsilon - \left(\frac{\pi}{a}\right)^2} \tag{10}$$

for $LSE_{1,n-1}$ modes [10].

It is evident from these equivalent circuit representations that the step discontinuity only couples energy between the waveguide modes but does not store energy. Energy storage is accomplished in the evanescent (reactive) fields excited

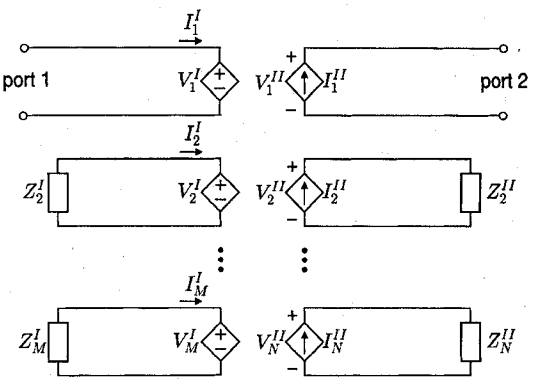


Fig. 2. Fullwave equivalent circuit of an $E$-plane and $H$-plane step discontinuity (waveguide $I$ has the larger aperture). The quantities $Z_k^{I,II}$ are the modal impedances of mode $k$ in waveguides $I$, $II$ given by (9) for $H$-plane steps and by (10) for $E$-plane steps, respectively. The gain coefficients $C_{mn}$ of the ideal dependent sources are given by the overlap integrals in (8). $M$ and $N$ modes are retained in waveguide $I$ and $II$, respectively.

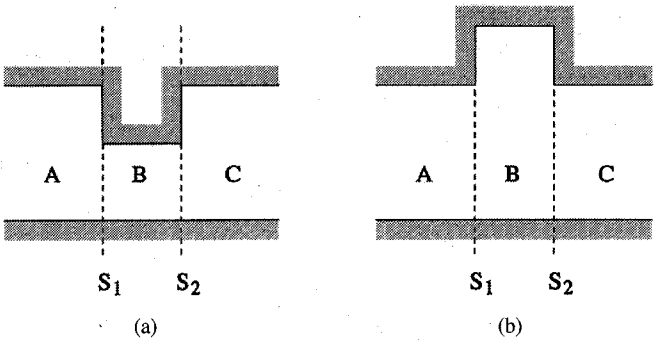


Fig. 3. Geometry of (a) a thick iris and (b) a stub discontinuity.

[1] In order to simplify the general notation for the equivalent multimode circuit models for $E$-plane and $H$-plane step discontinuities, the notation $LSE_{1,n-1}$ ($n = 1, 2, 3, \cdots$) instead of the more common notation $LSE_{1n}$ ($n = 0, 1, 2, \cdots$) is used here.

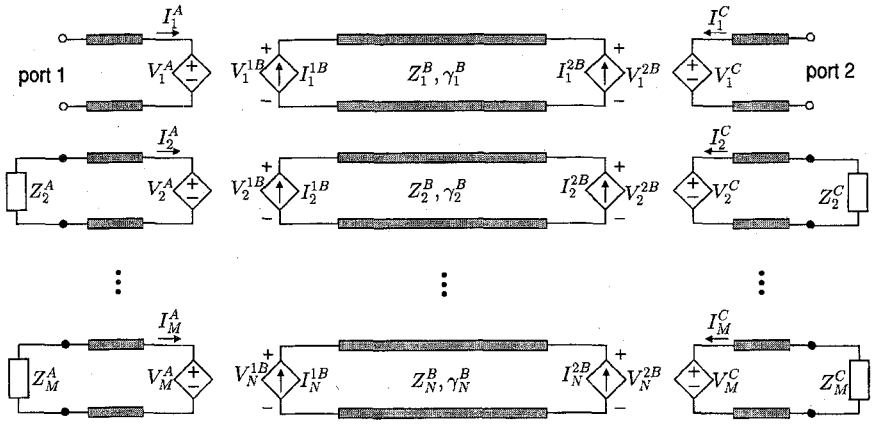


Fig. 4. Multimode equivalent circuit representation of a thick $E$-plane and $H$-plane iris. The dependent voltage and current sources are defined in (11)–(14). The impedance $Z_p^q$ and propagation constant $\gamma_p^q$ correspond to mode $p$ in region $q$, respectively, and are defined in the text for both $E$-plane and $H$-plane irises.

at the discontinuity which are represented in the equivalent circuit model in Fig. 2 by reactive modal impedances as terminations, i.e., by capacitive modal impedances for $E$-plane steps and inductive modal impedances for $H$-plane steps. Hence, the equivalent circuit model shown in Fig. 2 provides a fullwave description of both the $E$-plane and $H$-plane step discontinuity.

### B. Cascaded Steps

Many waveguide components including filters and phase shifters consist of cascaded step discontinuities. If the steps are sufficiently far apart, higher order modes excited at the two cascaded discontinuities do not couple and, hence, the "noninteracting" steps are connected only via one transmission line representing the dominant mode $TE_{10}$ mode. If the steps are "interacting," i.e., some of the higher order modes couple, the steps are connected via more than one transmission line.

Two examples of interacting steps which occur in many practical waveguide components are the thick iris and the stub discontinuity shown in Fig. 3. Both structures consist of two step discontinuities which are coupled through the dominant mode and one or more higher order modes. With reference to the thick iris in Fig. 3(a), the modal voltage and current amplitude coefficients representing the transverse electric and magnetic fields in region $A$ at interface $S_1$ are $V_m^A$ and $I_m^A$ $(m = 1, \cdots, M)$, respectively. Similarly, the voltage and current coefficients representing the transverse field amplitudes in region $B$ at interface $S_1$ are given by $V_n^{1B}$ and $I_n^{1B}$ $(n = 1, \cdots, N)$, respectively. The relationship between the amplitude coefficients at the step between waveguides $A$ and $B$ at interface $S_1$ is given by

$$V_m^A = \sum_{n=1}^{N} C_{mn}^I V_n^{1B}, \qquad (m = 1, \cdots, M) \tag{11}$$

$$I_n^{1B} = \sum_{m=1}^{M} C_{mn}^I I_m^A, \qquad (n = 1, \cdots, N) \tag{12}$$

where $C_{mn}^I$ represents the mode-coupling at the $S_1$ interface. Similarly, the voltage and current coefficients at the step discontinuity at interface $S_2$ are related by

$$V_m^C = \sum_{n=1}^{N} C_{mn}^{II} V_n^{2B}, \qquad (m = 1, \cdots, M) \tag{13}$$

$$I_n^{2B} = \sum_{m=1}^{M} C_{mn}^{II} I_m^C, \qquad (n = 1, \cdots, N) \tag{14}$$

where $C_{mn}^{II}$ represents the mode-coupling at the $S_2$ interface. For a symmetric iris or stub discontinuity, $C_{mn}^I = C_{mn}^{II}$.

The voltage and current coefficients at the two interfaces $S_1$ and $S_2$ for each waveguide mode in region $B$ are related through standard transmission line equations with characteristic impedances corresponding to the modal wave impedances given by (9) for $TE_{m0}$ modes ($H$-plane steps) and by (10) for $LSE_{1,n-1}$ modes ($E$-plane steps), respectively. The propagation constants are given by

$$\gamma_{m0}^B = \sqrt{\left(\frac{m\pi}{a_B}\right)^2 - \omega^2\mu\epsilon} \tag{15}$$

for $TE_{m0}$ modes, and

$$\gamma_{1n}^B = \sqrt{\left(\frac{\pi}{a_B}\right)^2 + \left[\frac{(n-1)\pi}{b_B}\right]^2 - \omega^2\mu\epsilon} \tag{16}$$

for $LSE_{1,n-1}$ modes. Similar equations are obtained for the stub discontinuity shown in Fig. 3(b).

As shown above, (11) and (12) lead to a simple multimode equivalent circuit description for the mode-coupling at the single step discontinuity at interface $S_1$ in terms of voltage-controlled voltage sources and current-controlled current sources. In the case of cascaded steps, the dependent sources in region $B$ are connected by "modal" transmission lines. The complete equivalent circuit representation of a thick (symmetric) iris is shown in Fig. 4 where the voltages and currents at interfaces $S_1$ and $S_2$ are given by (11)–(14).

The corresponding multimode equivalent circuit representation of the stub discontinuity is obtained by interchanging voltage and current sources at each interface.

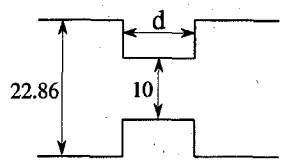


Fig. 5. Geometry of an inductive iris of variable thickness $d$ in a WR90 waveguide. Dimensions are given in mm.

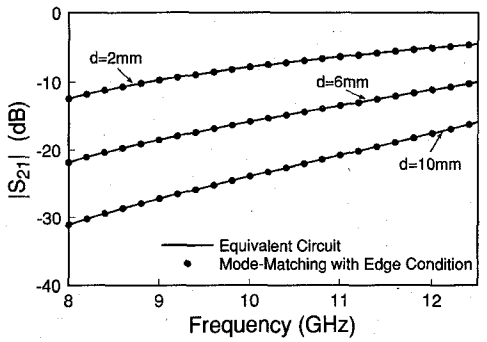


Fig. 6. Transmission coefficient of an inductive iris for different thicknesses $d$ as defined in Fig. 5.

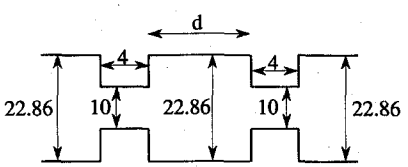


Fig. 7. Geometry of two cascaded inductive irises, separated by distance $d$. Dimensions are given in mm.

## III. Results

The new equivalent circuit approach has been implemented in the commercial microwave simulator Libra [6]. The accuracy of the multimode equivalent circuit model for both $E$-plane and $H$-plane steps [13] has been verified by comparison with other mode-matching solutions. In order to test the accuracy of the multimode equivalent circuit model for interacting steps, both single and cascaded irises and stub discontinuities are considered.

### A. Single and Cascaded Irises

The first case considers inductive irises of various thicknesses (Fig. 5), i.e., for various degrees of interaction between the steps via the higher order modes. Fig. 6 shows the transmission coefficient obtained by circuit simulation for different thicknesses $d$ of the iris. Also included in the figure are the results obtained from a mode-matching analysis which considers the correct edge behavior [8]. Perfect agreement between the two methods is obtained.

Fig. 7 shows the geometry of two cascaded inductive irises, separated by distance $d$. The transmission coefficient computed by circuit simulation is compared with results obtained with a mode-matching method [8], as shown in Fig. 8. Again, virtually perfect agreement between the two methods can be seen. Also included in the figure are the results for the case when the irises are defined as two-port circuit elements by

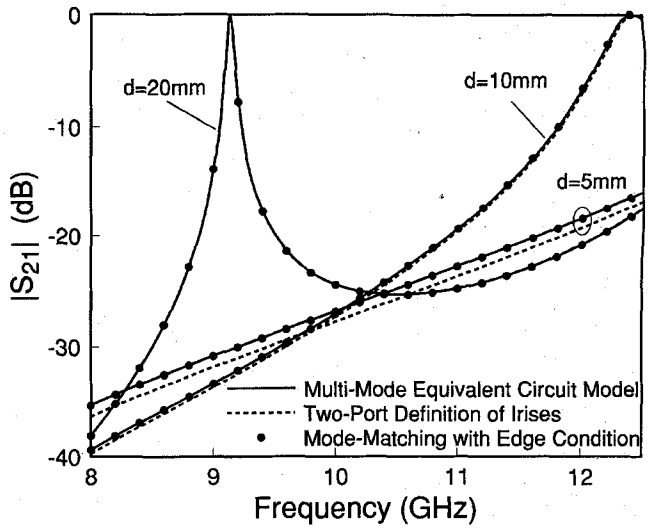


Fig. 8. Transmission coefficient for two cascaded inductive irises with dimensions as shown in Fig. 7.

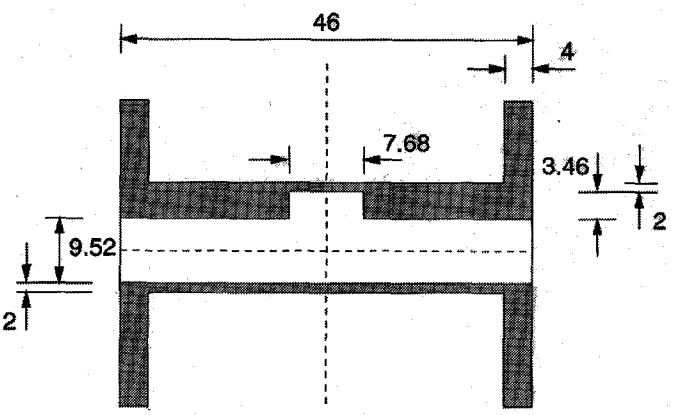


Fig. 9. Geometry of a single $E$-plane stub in a WR75 waveguide [8].

terminating all higher order modes in the wider regions in their modal impedances. In this case, the cascaded irises can interact only via the fundamental (propagating) $TE_{10}$ mode. As expected, interacting higher order modes can be neglected even for moderately separated irises ($d = 10$ mm) but must be included for correct analysis of closely spaced irises ($d = 5$ mm). The results shown in Fig. 8 also demonstrate the stability of the circuit simulation which dynamically decouples the higher order modes with increasing separation $d$ between the irises. This dynamic decoupling of higher order evanescent modes between interacting step discontinuities is a particularly attractive feature of the multimode equivalent circuit model approach as it produces an intrinsically stable analysis and design tool for waveguide components.

### B. Single and Cascaded Stub Discontinuities

Next, a single $E$-plane stub discontinuity in a rectangular waveguide and a structure containing three $E$-plane stubs are simulated and compared with the results obtained with the mode-matching technique in [8] which considers the correct edge behavior of the fields. The geometry of the single $E$-plane stub in a WR75 waveguide is illustrated in Fig. 9. The

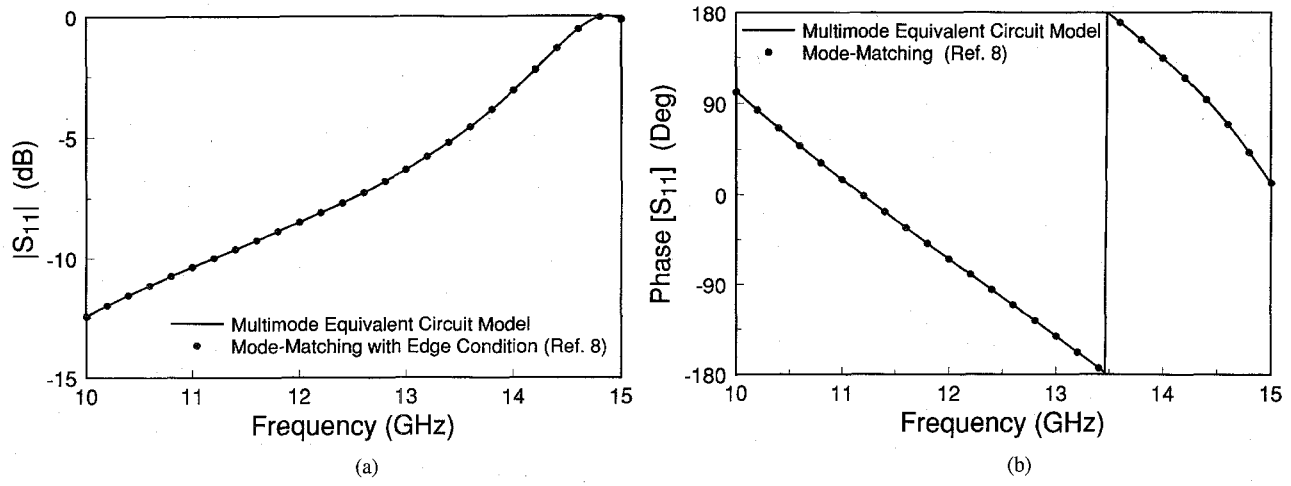


(a) (b)

Fig. 10. (a) Magnitude and (b) phase of the reflection coefficient of the $E$-plane stub discontinuity shown in Fig. 9.

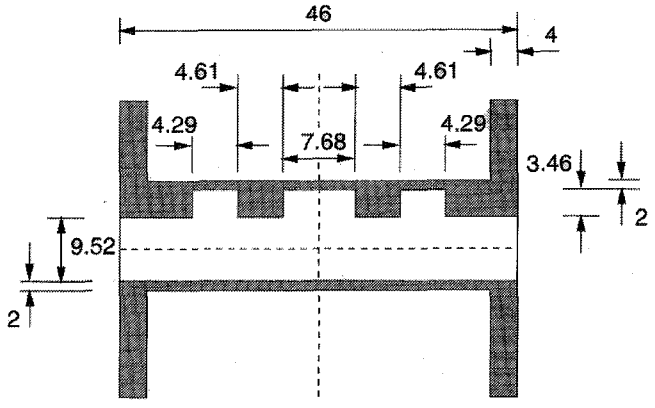


Fig. 11. Geometry of three cascaded $E$-plane stubs in a WR75 rectangular waveguide [8]. Dimensions are given in mm.

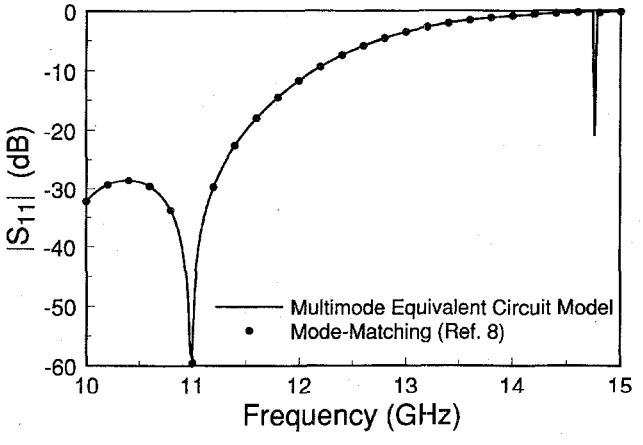


Fig. 12. Reflection coefficient of the $E$-plane stub discontinuity shown in Fig. 11.

magnitude and phase response of the reflection coefficient of the single $E$-plane stub obtained by circuit simulation is in excellent agreement with the results given in [8], as shown in Fig. 10.

The test waveguide structure containing three $E$-plane stubs is shown in Fig. 11. The simulated results of the reflection coefficient are plotted in Fig. 12. Again, the excellent agreement between the results obtained by circuit simulation and the

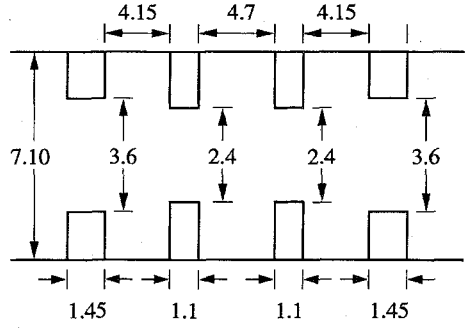


Fig. 13. Geometry of a bandpass filter for the Ka-band [14]. Dimensions are given in mm.

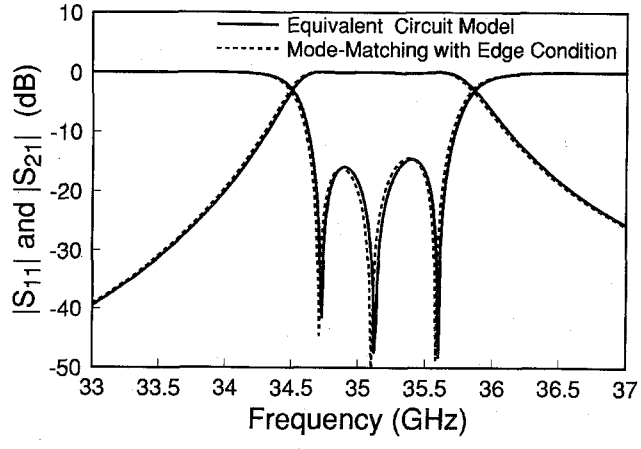


Fig. 14. Scattering parameters of a bandpass filter with dimensions given in Fig. 13.

mode-matching solution in [8] including the correct resolution of the main resonance at about 11 GHz is evident. It should be noted, however, that the second resonance close to 15 GHz predicted in the circuit simulation is not resolved by the mode-matching method in [8] but is present in the experimental data given in [8].

### C. Bandpass Filter

In the last application, the equivalent circuit approach has been implemented in Libra to analyze the bandpass filter designed in [14] for the Ka-band at 35 GHz and a bandwidth

of 1 GHz. The filter dimensions are given in Fig. 13. The results obtained by circuit simulation are shown in Fig. 14 and compared with the mode-matching method which includes the correct edge condition. The circuit simulation is performed by retaining ten modes in the wide regions, five modes in the irises of width 3.6 mm, and three modes in the irises of width 2.4 mm in order to avoid relative convergence problems [11]. The results obtained with the two different methods show very good agreement, thus validating the equivalent circuit approach for waveguide filter analysis and design.

## IV. Conclusion

New equivalent circuit models of single and cascaded $E$-plane and $H$-plane step discontinuities in a rectangular waveguide have been presented. The CAD-oriented equivalent circuit models enable fullwave analysis of a large class of waveguide components and circuits, including irises, stubs, filters, and phase shifters, on commercial microwave circuit simulators. The equivalent circuit models have been implemented on Libra to demonstrate their accuracy. Results of the circuit analysis were found to be virtually in perfect agreement with solutions obtained with the standard mode-matching technique based on incident and reflected wave amplitudes and a mode-matching technique which includes the correct edge behavior of the fields.

The potential benefits of implementing the proposed equivalent circuit model in commercial circuit simulators include the direct and full use of available design, optimization, and graphical user interface capabilities of the CAD tool. In addition, implementation of the fullwave analysis and design tool entirely inside a circuit simulator should offer other performance advantages over existing waveguide CAD tools.

## Appendix

The normalized transverse field solutions for $TE_{m0}$ modes in a rectangular waveguide of width $a$ and height $b$ are given by [10]

$$\phi_m(x, y) = \sqrt{\frac{2}{ab}} \sin\left(\frac{m\pi}{a}x\right). \tag{17}$$

The coupling coefficient $C_{mn}$ between mode $m$ in waveguide $I$ of width $a_1$ and mode $n$ in waveguide $II$ of width $a_2$ $(a_1 \geq a_2)$ is

$$C_{mn} = \frac{2}{\sqrt{a_1 a_2}} \int_0^{a_2} \sin\left(\frac{m\pi}{a_1}x\right) \sin\left(\frac{n\pi}{a_2}x\right) dx. \tag{18}$$

The normalized transverse field solutions for $LSE_{1,n-1}$ modes ($TE_x$ modes) $(n = 1, 2, 3, \cdots)$ in a rectangular waveguide of width $a$ and height $b$ are [10]

$$\phi_n(x, y) = \sqrt{\frac{2\delta_n}{ab}} \sin\left(\frac{\pi}{a}x\right) \cos\left[\frac{(n-1)\pi}{b}y\right] \tag{19}$$

where

$$\delta_n = \begin{cases} 1, & n = 1 \\ 2, & n > 1. \end{cases} \tag{20}$$

The corresponding coupling coefficient $C_{mn}$ between mode $m$ in waveguide $I$ of height $b_1$ and mode $n$ in waveguide $II$ of height $b_2$ $(b_1 \geq b_2)$ is

$$C_{mn} = \sqrt{\frac{\delta_m \delta_n}{b_1 b_2}} \int_0^{b_2} \cos\left[\frac{(m-1)\pi}{b_1}y\right] \cdot \cos\left[\frac{(n-1)\pi}{b_2}y\right] dy. \tag{21}$$

## References


[1] HFSS—High Frequency Structure Simulator (software package), Hewlett-Packard Co.

[2] T. Itoh, Ed., *Numerical Techniques for Microwave and Millimeter–Wave Passive Structures.* New York: Wiley, 1989.

[3] F. Alessandri, G. Bartolucci, and R. Sorrentino, "Admittance matrix formulation of waveguide discontinuity problems: Computer-aided design of branch guide directional couplers," *IEEE Trans. Microwave Theory Tech.*, vol. 36, pp. 394–403, Feb. 1988.

[4] H. Patzelt and F. Arndt, "Double-plane steps in rectangular waveguides and their application for transformers, irises, and filters," *IEEE Trans. Microwave Theory Tech.*, vol. MTT-30, pp. 771–776, May 1982.

[5] N. Marcuvitz, *Waveguide Handbook.* Lexington, MA: Boston Tech. Pub., 1964.

[6] HP EEsof, Westlake Village, CA.

[7] F. Alessandri, M. Mongiardo, and R. Sorrentino, "Computer-aided design of beam forming networks for modern satellite antennas," *IEEE Trans. Microwave Theory Tech.*, vol. 40, no. 6, pp. 1117–1127, June 1992.

[8] T. Rozzi and M. Mongiardo, "$E$-plane steps in rectangular waveguide," *IEEE Trans. Microwave Theory Tech.*, vol. 39, pp. 1279–1288, Aug. 1991.

[9] R. E. Collin, *Field Theory of Guided Waves,* 2nd ed. New York: IEEE Press, 1991, ch. 6 and 8.

[10] R. F. Harrington, *Time—Harmonic Electromagnetic Fields.* New York: McGraw-Hill, 1961, ch. 4.

[11] S. W. Lee, W. R. Jones, and J. J. Campbell, "Convergence of numerical solutions of iris-type discontinuity problems," *IEEE Trans. Microwave Theory Tech.*, vol. MTT-19, pp. 528–536, June 1971.

[12] V. K. Tripathi and J. B. Rettig, "A SPICE model for multiple coupled microstrips and other transmission lines," *IEEE Trans. Microwave Theory Tech.*, vol. MTT-33, pp. 1513–1518, Dec. 1985.

[13] A. Weisshaar, M. Mongiardo, and V. K. Tripathi, "CAD-oriented equivalent circuit modeling of step discontinuities in rectangular waveguide," *IEEE Microwave Guided Wave Lett.*, vol. 6, no. 4, Apr. 1996.

[14] W. Menzel, F. Alessandri, M. Mongiardo, R. Sorrentino, C. Eswarappa, P. P. M. So, and W. J. R. Hoefer, "Analysis of a millimeter–wave filter using transmission line matrix and mode matching methods and comparison with the measurements," in *Proc. 9th Annu Rev. Progress Appl. Computational Electromagn,* Monterey, CA, Mar. 1993, pp. 289–296.

[15] F. Alessandri, M. Dionigi, and R. Sorrentino, "A fullwave CAD tool for waveguide components using a high speed direct optimizer," *IEEE Trans. Microwave Theory Tech.*, vol. 43, no. 9, pp. 2046–2052, Sept. 1995.


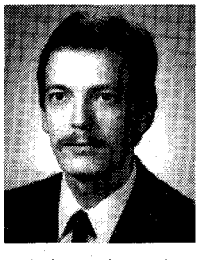


**Andreas Weisshaar** (S'90–M'91) received the Diplom-Ingenieur (Dipl.-Ing.) degree in electrical engineering from the University of Stuttgart, Germany, in 1987, and the M.S. and Ph.D. degrees in electrical and computer engineering from Oregon State University, Corvallis, in 1986 and 1991, respectively.

Since 1992, he has been an Assistant Professor at the Department of Electrical and Computer Engineering at Oregon State University. He has been engaged in the development of computational techniques for and modeling of guided-wave structures for microwave and millimeter–wave circuits, integrated and fiber optics, and quantum waveguide devices. His current research interests are in the areas of microwave circuits, fiber optic transmission systems, and wireless communications.

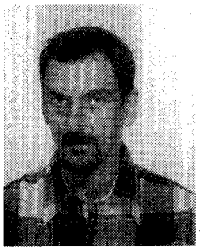

**Mauro Mongiardo** (M'91) is an Associate Professor at the University of Perugia in Italy. He has received the Laurea degree from the University of Rome (summa cum laude) and the Ph.D. from the University of Bath, United Kingdom. He has been a visiting scientist at the University of Victoria, BC, Canada, at the University of Bath, at Oregon State University, Corvallis, and at the Technical University of Munich, Germany.

From 1983 to 1988, he was engaged in microwave radiometry, inverse problems, and in the experimental validation of a four-channel radiometer developed for temperature retrieval of biological bodies. His main contributions are in the area of modeling of waveguide discontinuities, both in the cases of closed waveguides and open waveguides such as microstrip lines or coplanar waveguides. Considerable interest has also been devoted to numerical methods with contributions in the areas of mode-matching techniques, integral equations, variational techniques, FDTD, TLM, and FEM. He is active in the frequency and time–domain analysis of MMIC and he is currently interested in the modeling and computer-aided procedures for the design of microwave and millimeter wave components.

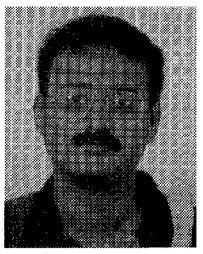

**Alok Tripathi** (S'96) received the B. Tech with distinction from H. B. Technological Institute, Kampur, India, in 1990, and M.Sc. in electrical engineering from Indian Institute of Science, Bangalore, India, in 1994. He is currently enrolled as a Ph.D. student in the Electrical and Computer Engineering program at Oregon State University, Corvallis.

His research interests include CAD and modeling of RF circuits and packages and numerical techniques in electromagnetics.

**Vijai K. Tripathi** (M'68–F'93) received the B.Sc. degree from Agra University, India, M.Sc. Tech. degree in electronics and radio engineering from Allahabad University, India, and the M.S.E.E. and Ph.D. degrees in electrical engineering from the University of Michigan, Ann Arbor, in 1958, 1961, 1964, and 1968, respectively.

He is Professor and Head of Electrical and Computer Engineering at Oregon State University, Corvallis. Prior to joining Oregon State in 1974, he had been with the Indian Institute of Technology, Bombay, the University of Michigan, Ann Arbor, and the University of Oklahoma, Norman. His visiting and sabbatical appointments include the Division of Network Theory at Chalmers University of Technology, Gothenburg, Sweden in 1981–1982, Duisburg University, Duisburg, West Germany in 1982, the Naval Research Laboratory, Washington, DC in 1984, and the University of Central Florida, Orlando, in Fall 1990. Over the years he has been a consultant to many industrial organizations including AVANTEK, EEsof Inc., Teledyne MMIC, and Tektronix. His research activities are in the general areas of microwave and distributed parameter circuits, applied electromagnetics and electronic packaging, and interconnect technologies.